Partition of unity methods for approximation of point water sources in porous media

Pavel Exner[a,*], Jan Březina[a]

[a] *Technical University of Liberec, Studentská 1402/2, 461 17 Liberec 1, Czech Republic*

Abstract

In this work we demonstrate usage of Partition of Unity (PU) methods to improve approximation of singularities in the solution of the Poisson equation. Our model describes a steady flow of water in a system of aquifers which consist of porous media. The aquifers are perforated by wells and boreholes which are often represented as point sources considering their small diameter in comparision with the vast size of the aquifer. This brings singularities into the solution. The extended and stable generalized finite element method (XFEM and SGFEM) were implemented to solve the problem and a proper adaptive integration strategy was developed to gain optimal convergence rates.

Keywords: PUM, XFEM, SGFEM, adaptive integration, point sources

1. Introduction

People often consider in their models of flow in porous media very large areas which can contain various phenomena of very small scale compared with the size of the areas. These can be some disruptions of the porous media, e.g. cracks and wells, or material inhomogeneities that cause large gradients in pressure head and velocity or even their discontinuities.

Using the standard finite element method (FEM) we are unable to properly approximate the quantities in the vicinity of these disturbances, unless

*Corresponding author.

Email addresses: pavel.exner@tul.cz (Pavel Exner), jan.brezina@tul.cz (Jan Březina)

URL: https://github.com/Paulie14/xfem_project (Pavel Exner)

we introduce elements of the same scale in the mesh. This leads to higher requirements on mesh processing (refinement) and increase of computational costs due to growing number of degrees of freedom.

In this work we use PU (Partition of Unity) methods to overcome these problems and demonstrate it on a steady two-dimensinal aquifer model containing hydro-geological wells which cause singularities in solution. We follow the work [1] and [2] who have already used the XFEM (eXtended FEM) on a similar model. However, we focus mainly on the study of the PU methods. In particular, we use the XFEM and its corrected version (including ramp function and shift), e.g. [3], and the SGFEM, [4] and [5]. We are able to measure the convergence of pressure in L^2 norm over the aquifer domain and we compare the used methods. We also investigate the error of the adaptive integration on the enriched elements and introcude improvement. In addition, we suggest better choice of enrichment area based on a tolerance criterion.

The implementation was done in C++ language using the Deal II library [6], the finite element library. which does not support any enrichment techniques at the moment.

We describe the model in the beginning of the article, set the problem and go through the PU methods in more details. Then we show some numerical aspects of the problem which we must deal with, especially the adaptive integration in section 4. Results, convergence of methods and conditioning of the algebraic system are discussed right after and further research goals are pointed out at the end.

2. Model

We consider a steady flow in a system of aquifers (2D layers of given thickness) which are separated by impermeable layers (aquitards). The aquifers are connected by wells which act as sources or sinks in the domain of each aquifer. The pressure in the aquifers is further governed by the boundary condition of the aquifers which can be of Dirichlet type or be homogenous of Neumann type.

We describe the wells as interior boundary condition therefore we need to define the computational domain as the aquifer domain with wells cross-sections cut off. Let the Θ^m be the domain on m-th aquifer, $m = 1, \dots M$, B_w^m be its cross-section with w-th well, $w \in \mathcal{W} = \{1, \dots, W\}$, and denote the union $B^m = \bigcup_w B_w^m$. We then define domain $\Omega^m = \Theta^m \setminus B^m$ with an

exterior boundary consisting of exclusive parts $\partial\Theta^m = \Gamma_D^m \cup \Gamma_N^m$ and an interior boundary $\partial B^m = \bigcup_w \partial B_w^m$, such that $\partial\Omega^m = \partial\Theta^m \cup \partial B^m$.

The distribution of the pressure head in m-th aquifer is described by Poisson equation and boundary conditions

$$\begin{aligned}
\nabla \cdot (-\mathbf{T}^m \nabla h^m) &= f^m \qquad \text{on } \Omega^m \subset \mathbf{R}^2,\ \forall m = 1, \ldots, M, && (1)\\
h^m|_{\Gamma_D^m} &= h_D^m, && (2)\\
(-\mathbf{T}^m \nabla h^m \cdot \boldsymbol{n})\,|_{\Gamma_N^m} &= 0, && (3)\\
(-\mathbf{T}^m \nabla h^m \cdot \boldsymbol{n})\,|_{\partial B_w^m} &= q_w^m \qquad \forall w \in \mathcal{W}, && (4)
\end{aligned}$$

where $\mathbf{T}^m\,[\mathrm{m^2 s^{-1}}]$ denotes the transmisivity tensor, $h^m\,[\mathrm{m}]$ the pressure head, $f^m\,[\mathrm{ms^{-1}}]$ source density, $\boldsymbol{n}$ unit normal vector on the boudnary and $q_w^m = Q_w^m/|\partial B_w^m|$ is the density of the flow from the well to the aquifer over the well boundary ∂B_w^m. Equation (1) is derived from the Darcy law and the continuity equation for incompressible fluid.

Presuming the aquitards to be fully impermeable, the communication between aquifers is possible only through wells. We can prescribe the flow balance equation

$$\begin{aligned}
Q_w^m &= Q_{w,in}^m - Q_{w,out}^m, \text{ where} && (5)\\
Q_w^m &\ \ldots \text{ flow into aquifer across the well boundary,}\\
Q_{w,in}^m &\ \ldots \text{ flow from upper aquifer,}\\
Q_{w,out}^m &\ \ldots \text{ flow into lower aquifer.}
\end{aligned}$$

Fig.1 presents the equation (5) and denotes the flows $Q_{w,\cdot}^m$ by red arrows. We can look at the flows in the balance equation as 1D problems which are governed by a difference of pressure heads and a transition coefficient. Using this idea, we can substitute the flows in the equation (5) and get

$$\int_{\partial B_w^m} \sigma_w^m \left(h^m - H_w^m\right)\,\mathrm{d}s = c_w^{m+1}\left(H_w^m - H_w^{m+1}\right) - c_w^m\left(H_w^{m-1} - H_w^m\right), \qquad (6)$$
$$\forall m = 1, \ldots, M \text{ and } \forall w \in \mathcal{W},$$

where $\sigma_w^m\,[\mathrm{ms^{-1}}]$ denotes the permeability coefficient between w-th well and m-th aquifer, H_w^m the pressure head in the well w at the level of m-th aquifer and finally $c_w^m\,[\mathrm{m^2 s^{-1}}]$ is the permeability of the well w through aquitard m.

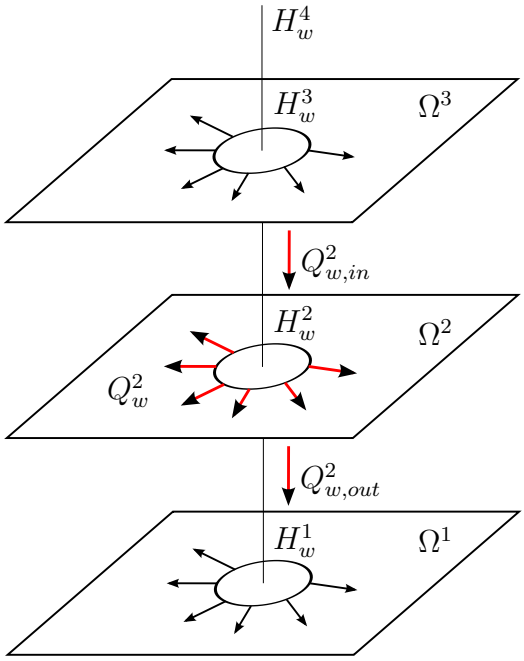

Figure 1: Flow balance in the well.

The problem is now to find set of functions $h^m \in C^2(\Omega^m) \cap C^1(\bar{\Omega}^m)$ and set of pressure values in the wells $H_w^m \in \mathbf{R}$, for all $m \in \{1, \ldots, M\}$ and $w \in \mathcal{W}$ that satisfy the equations (1) and (6).

Note that if the lower end of well is considered isolated from below, the coefficient must be set $c_w^1 = 0$. With $c_w^m = 0$ we can also simulate the end of the well w at the level of aquifer m.

We mention yet the equation (6) for $m = M + 1$ which is one level above the upmost aquifer and is adjusted to the form

$$c_w^M \left(H_w^M - H_w^{M+1} \right) = 0. \tag{7}$$

The pressure at the top of the well H_w^{M+1} can be set as an input value or, if not set, is gained as part of the solution from the equation (7), see H^4 in Fig.1.

The boundary term in (6) with large σ_w^m would force the pressure head along the well edge to be constant (equal H_w^m), which cannot be in general

satisfied. Therefore it is weakened and later replaced by the average

$$\langle h^m \rangle = \frac{1}{|\partial B_w^m|} \int\limits_{\partial B_w^m} h^m \, \mathrm{d}s, \tag{8}$$

which corresponds to [1].

2.1. Weak formulation

We define the trial and the test spaces

$$V = \prod_{m=1}^{M} \left(H^1(\Omega^m) \times \mathbf{R}^W \right), \tag{9}$$

$$V_0 = \prod_{m=1}^{M} \left(H_0^1(\Omega^m) \times \mathbf{R}^W \right), \tag{10}$$

where H^1 and H_0^1 are standard Sobolev spaces and

$$H_0^1(\Omega^m) = \{ \varphi \in H^1(\Omega^m); \varphi|_{\Gamma_D^m} = 0 \}.$$

We can now introduce the weak solution u and test functions v

$$u = (h^1, \ldots, h^M, H_1^1, \ldots, H_W^{M+1}) \in V, \tag{11}$$

$$v = (\varphi^1, \ldots, \varphi^M, \Phi_1^1, \ldots, \Phi_W^{M+1}) \in V_0. \tag{12}$$

To obtain the weak form we apply the standard Galerkin method on (1) and (6), we further substract the second equation from the first one, use (8) and get for $m = 1, \ldots, M$

$$\int\limits_{\Omega^m} T^m \nabla h^m \cdot \nabla \varphi^m \, \mathrm{d}\boldsymbol{x} + \sum_{w \in \mathcal{W}} \sigma_w^m \left(\langle h^m \rangle - H_w^m \right) \left(\langle \varphi^m \rangle - \Phi_w^m \right) + \\ + \sum_{w \in \mathcal{W}} \left[c_w^{m+1} \left(H_w^m - H_w^{m+1} \right) \Phi_w^m - c_w^m \left(H_w^{m-1} - H_w^m \right) \Phi_w^m \right] = \\ = \int\limits_{\Omega^m} f^m \varphi^m \, \mathrm{d}\boldsymbol{x}. \tag{13}$$

3. Discretization

We can now proceed to the choice of the enrichment and discretize the system of equations (13). Let's imagine that we have only one aquifer so we can omit the upper index m in this section. In fact, it is appropriate to do so in some notations of shape functions because we do consider the same triangulation for every aquifer in our implementation.

3.1. Enrichment function

The enrichment function in general can be obtained from the knowledge of the solution character or from the solution of a simple local problem which will provide us the function. In our case the simple problem is finding pressure distribution in a circular domain Ω with one well placed at the center. It can be easily proved that the function

$$h = a \log(r_w) + b \tag{14}$$

is the solution of a Laplace equation $-T\Delta h = 0$, just by putting the function into the equation. Argument r_w of the logarithm is the distance from the well center

$$r_w(\boldsymbol{x}) = \|\boldsymbol{x} - \xi_w\| = \sqrt{(x - x_w)^2 + (y - y_w)^2}.$$

We see in (14) the logarithmic dependence of the pressure head on the distance from the well. If we represented the well only by a point, the pressure head would go to infinity while closing to the point (singularity $\lim_{r\to 0} \log r = -\infty$). Instead, we keep in mind the radius of the well R_w and introduce (global) enrichment function

$$s_w(\boldsymbol{x}) = \begin{cases} \log(r_w(\boldsymbol{x})), & r_w > R_w \\ \log(R_w), & r_w \leq R_w \end{cases}. \tag{15}$$

See Fig.2. It is natural to use the same set of s_w on each aquifer since they depends only on r_w and the wells are placed at the same positions throughout the aquifers (we consider only vertical wells, perpendicular to aquifers).

3.2. Partition of unity methods

Let $N_\alpha(\boldsymbol{x})$, $\alpha \in \mathcal{I} = \{1, \ldots, N\}$ be the standard linear finite element shape functions associated with the node $\boldsymbol{x}_\alpha$ of the triangulation. In **standard XFEM**, we write the solution in the form

$$h(\boldsymbol{x}) = \sum_{\alpha\in\mathcal{I}} a_\alpha N_\alpha(\boldsymbol{x}) + \sum_{w\in\mathcal{W}} \sum_{\alpha\in\mathcal{I}_w^e} b_{\alpha w} \phi_{\alpha w}(\boldsymbol{x}), \tag{16}$$

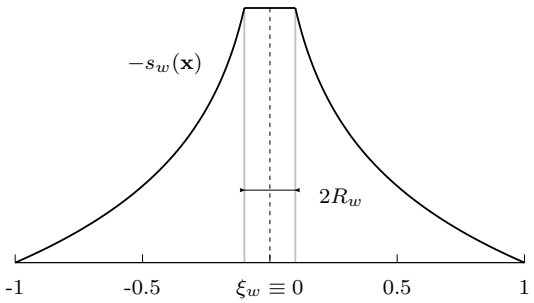

Figure 2: The enrichment function.

where a_α are the standard FE degrees of freedom and $b_{\alpha w}$ are degrees of freedom coming from enrichment of the well w. The index set $\mathcal{I}_w^e$ includes all nodes enriched by the well w, which means that we have several enrichment functions and each can enrich different nodes. The local enrichment functions $\phi_{\alpha w}$ in (16) are defined in the following way

$$\phi_{\alpha w} = N_\alpha(\boldsymbol{x}) L_{\alpha w}(\boldsymbol{x}), \quad \alpha \in \mathcal{I}_w^e, w \in \mathcal{W}, \tag{17}$$

where simply the enrichment function $L_{\alpha w}(\boldsymbol{x}) = s_w(\boldsymbol{x})$.

3.2.1. Corrected XFEM

The corrected XFEM [3] deals with the convergence problem on blending elements and introduces the **ramp function**

$$\begin{aligned} G_w(\boldsymbol{x}) &= \sum_{\alpha \in \mathcal{I}_w^e} N_\alpha(\boldsymbol{x}) \\ &= \begin{cases} 0 & \text{on unenriched elements} \\ 1 & \text{on elements where all nodes are enriched} \\ ramp & \text{on elements where some of the nodes are enriched} \end{cases} \end{aligned} \tag{18}$$

It also extends the set of enriched nodes, denoted by $\mathcal{J}^e$, by enriching (unenriched) nodes on elements, where only some of the nodes are in $\mathcal{I}^e$. Thus $\mathcal{I}^e \subset \mathcal{J}^e$ and there are more enriched nodes. The enrichment function changes into the form

$$L_{\alpha w} = G_w(\boldsymbol{x}) s_w(\boldsymbol{x}), \quad \alpha \in \mathcal{J}^e, w \in \mathcal{W}. \tag{19}$$

They further suggests the **shifted** enrichment functions in order to preserve the property of standard FE approximation at nodes $h(\boldsymbol{x}_\alpha) = a_\alpha$; the value

at the node is equal the corresponding degree of freedom. The enrichment functions must be then zero at the nodes which is satisfied in the form

$$L_{\alpha w} = G_w(\boldsymbol{x}) \left[s_w(\boldsymbol{x}) - s_w(\boldsymbol{x}_\alpha) \right], \quad \alpha \in \mathcal{J}^e, w \in \mathcal{W}. \tag{20}$$

The property of the shifted formulation enables us to prescribe Dirichlet boundary condition such that $a_\alpha = h_D(\boldsymbol{x}_\alpha)$.

For the purpose of this article, let's call the XFEM with ramp function **XFEM-r** and the shifted version **XFEM-s**, as we shall reference to them later.

3.2.2. SGFEM

Finally we present the **SGFEM**, according to [5]. The enrichment function is defined as the substraction of the global enrichment function and its interpolation

$$L_{\alpha w} = \left[s_w(\boldsymbol{x}) - \pi_\tau(s_w)(\boldsymbol{x}) \right], \quad \text{on } \tau,\ \alpha \in \mathcal{I}^e, w \in \mathcal{W}. \tag{21}$$

where the interpolantion π_τ is built using the finite element shape functions associated with nodes $\mathcal{I}(\tau)$ of the element τ

$$\pi_\tau(s_w)(\boldsymbol{x}) = \sum_{\beta \in \mathcal{I}(\tau)} s_w(\boldsymbol{x}_\beta) N_\beta(\boldsymbol{x}). \tag{22}$$

Of course $\alpha \in \mathcal{I}(\tau)$ in (21). Notice that there are no additional enriched nodes on blending elements, like in $\mathcal{J}^e$ in (19) and (20), and no ramp function is involved.

4. Integration on enriched elements

In order to compute the entries of the system matrix, we need to integrate the expressions containing the enrichment functions. These of course can be non-polynomial, like they are in our case. The standard quadrature rules are not appropriate any more, as they are constructed to integrate precisely polynomials up to a given degree. The higher requirements on integration precision are the price for using enrichment functions and a coarse mesh.

There are two aspects which the integration must handle properly:

- the steep gradient of the pressure head in the vicinity of a well (the singularity),

- the well edge (since the elements of the triangulation do not take the well into account)

One of the approaches to improve integration is local element refinement. We remind that the refinement only enables placing more quadrature points in the element and does not bring any more degrees of freedom in the system. We will discuss the criterions for adaptive refinement, suggest improvement and compare our solution with the original one in this subsection. We will refer also some of the convergence results which will be shown later in 6.

4.1. Adaptive refinement of an element

[1] used a criterion for adaptive refinement according to which only the subelements that have nonzero cross-section with the well are refined. This catches nicely the well edge but it can work well only in some special cases when the well is at the node of an element or near the center of an element. The problem comes when the well is placed near the edge or node of an element. In that case there can be large difference in the size of neighbouring subelements as you can see in Fig.3a. Although the integrand is computed precisely enough on the element with the well inside, the quadrature points on the neighbouring elements (where the pressure head gradient can be still large) are placed very sparsely and the integration error is large.

We suggested additional criterion for subelements refinement which takes into account a subelement diameter and its distance from the well

$$d_T > C_R|d_{min} - r_w|, \tag{23}$$

where d_T is the diameter of the subelement and d_{min} is minimal distance between a vertex of the subelement and the well edge. C_R is a scaling constant, equal 1.0 by default, through which we can control the significance of the criterion.

In this way, the elements in which the well does not lie are also refined as you can see in Fig.3b. The quadrature points are then distributed more 'smoothly' around the well and the integrals with gradients can be computed more accurately.

In Fig.4 you can see the L_2 norms of the error on the enriched elements which were computed also using the corresponding adaptive integration. Notice the scale of the improved version – the error on elements is in small range and is not significantly concentrated anywhere. On the other hand, the original version shows out large error that is concentrated on the closest non-refined element to the well.

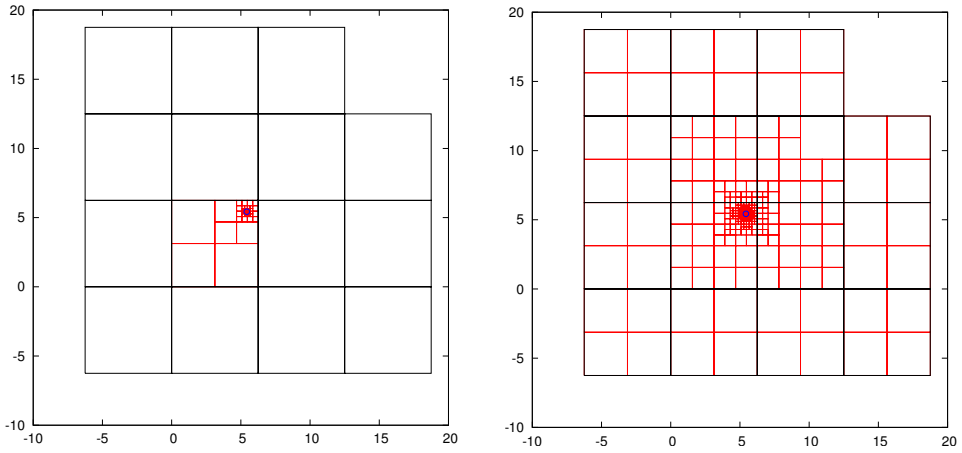

(a) original refinement (b) improved refinement

Figure 3: Comparision of the original and improved refinement techniques. Black lines denote enriched element edges, red lines denote adaptive refinement (subelement edges) and the well edge is blue.

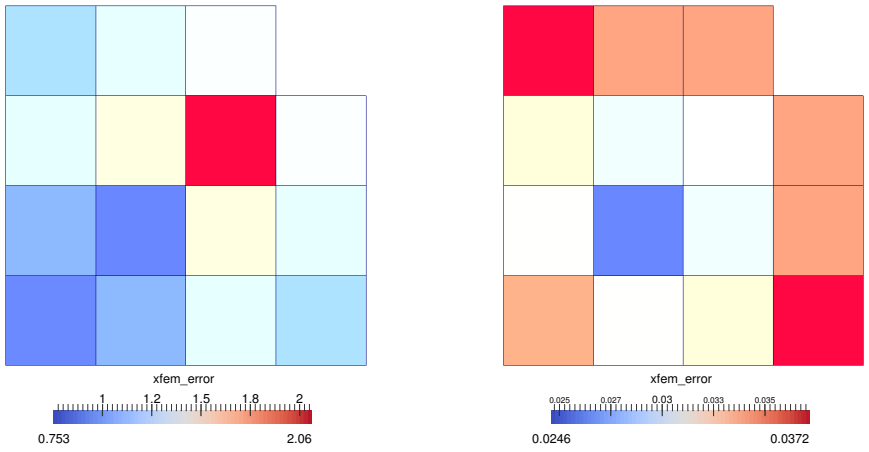

(a) original refinement (b) improved refinement

Figure 4: Comparision of elementwise error in L_2 norm using different refinement techniques.

4.2. Circle integration experiment

The approximation of the integration domain is also the source of the error. We decided to run an experiment on integrating the characteristic

function of the well with our adaptive integration. The domain Ω is a square 4×4 out of which a circle of radius 1.0 is cut off. The characteristic function is considered

$$\chi(\boldsymbol{x}) = \begin{cases} 0 & \text{if } \boldsymbol{x} \text{ is inside the circle} \\ 1 & \text{otherwise} \end{cases} \tag{24}$$

and the integral

$$\int_{\Omega} \chi(\boldsymbol{x}) \, \mathrm{d}\boldsymbol{x} = 4^2 - \pi \tag{25}$$

is equal the area of the square minus the area of the circle.

In this experiment we investigate the influence of the order of the quadrature rule and the level of the refinement on how precisely the well geometry is captured.

In the graph in Fig.5 we can see that for all the quadratures the convergence rate is similar, around 1.5. The gain from using higher order quadratures is not worth, especially in case of the order 4 the error is not much smaller than the error of the quadrature of the order 3.

Finally the highest level of refinement is chosen to be 10 and the quadrature order to be 3. The number of the quadrature points generated by the process desribed above in 4.1 is then similar both in the original (14793) and improved version (14819).

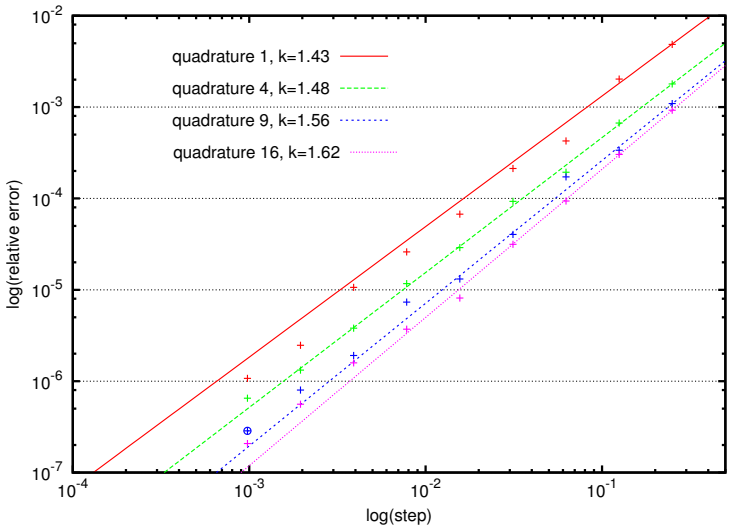

Figure 5: Convergence of adaptive refinement of a circle cutoff.

5. Estimate the enrichment radius

The enrichment is done in order to diminish approximation error of the precise solution of the problem, i.e. $\tilde{e}_h = \min_{u_h \in V_h} \|u - u_h\|_V$. Let us consider a well at origin, the radius R of the enrichment should be chosen so that

$$\min_{u_h \in V_h^P} \|\log \boldsymbol{x} - u_h\|_{V(\Omega^P)} \leq \epsilon$$

where V_h^P is polynomial finite element approximation space on unenriched part Ω^P of the domain Ω, $V = H^1(\Omega)$, and ϵ is prescribed tolerance.

For linear elements and 1D case, we get

$$\begin{aligned}\|\log x - u_h\|^2_{L^2(r,r+h)} &= h \int_0^1 \left|\log(r+ht) - \left[(1-t)\log r + t\log(r+h)\right]\right|^2 \mathrm{d}t \\ &= \frac{h^5}{4r^4}\int_0^1 t^2(1-t)^2 + O(h^6) \approx \frac{h^5}{120r^4}\end{aligned}$$

$$\begin{aligned}\|\nabla(\log x - u_h)\|^2_{L^2(r,r+h)} &= h \int_0^1 \left|\frac{1}{r+ht} - \frac{\log(r+h) - \log r}{h}\right|^2 \mathrm{d}t \\ &= \frac{h^3}{r^4}\int_0^1 (\frac{1}{2} - t)^2 + O(h^4) \approx \frac{h^3}{12r^4}\end{aligned}$$

And thus,

$$\|\log x - u_h\|_{H^1(r,r+h)} \approx h^{3/2} r^{-2} 12^{-1/2}.$$

Let us consider a 2D domain. The H^1 error on elements in distance r is same as in the 1D case up to a constant close to 1 (potrebuje numericke overeni). Thus error on the band at distance r is proportional to

$$\|\log \boldsymbol{x} - u_h\|^2_{H^1(\Omega^P)} \approx \int_R^{diam\Omega} 2\pi r \frac{h^3}{12r^4}\mathrm{d}r \leq \frac{2\pi h^3}{12}\frac{2}{R^2} \approx \frac{h^3}{R^2}.$$

Then, the optimal choice of R for given H^1 tolerance ϵ should be

$$R = \frac{h^{3/2}}{\epsilon}$$

6. Results

6.1. Analytical solution

To measure convergence an analytic solution is needed. Let's start with a Laplace problem on a circular disk with a single well in the center

$$\begin{aligned} -T\Delta h &= 0 \\ h|_{\partial\Omega} &= P_D \\ h|_{B_w} &= P_w \end{aligned} \tag{26}$$

where the pressure P_w at the well edge B_w and the pressure P_D at the boundary are given. Remind the function (14) $h = \log(r_w) + b$ (which we used to define the enrichment function) and find the constants a, b using the boundary conditions such that (14) is the solution of (26). We obtain a, b by solving

$$\begin{aligned} a\log(R_w) + b &= P_w, \\ a\log(R) + b &= P_D, \end{aligned}$$

where R is radius of the domain and R_w is the well radius. The solution of (26), which we shall use as the reference, is then

$$h = a\log(r_w) + b \qquad \text{with } a = \frac{P_w}{\log\left(\frac{R_w}{R}\right)},\ b = -a\log R \tag{27}$$

Second problem we solve is a Poisson problem

$$\begin{aligned} -T\Delta h &= TU\omega^2\sin(\omega x) \\ h|_{\partial\Omega} &= P_D + U\sin(\omega x) \\ h|_{B_w} &= P_w. \end{aligned} \tag{28}$$

where U and ω are given and the solution

$$h = a\log(r_w) + b + U\sin(\omega x), \tag{29}$$

with a, b being the same as in (27), is obtained the same way as above.

8. Acknowledgement

This work was made under the sincere guidance and support of Mgr. Jan Březina, Ph.D.

This work was supported by the Ministry of Education of the Czech Republic within the SGS project no. 21066/115 on the Technical University of Liberec.

[1] R. Gracie, J. R. Craig, Modelling well leakage in multilayer aquifer systems using the extended finite element method, Finite elements in Analysis and Design, Elsevier B.V. 46 (2010) 504–513.

[2] J. R. Craig, R. Gracie, Using the extended finite element method for simulation of transient well leakage in multilayer aquifers, Advances in Water Recources, Elsevier B.V. 34 (2011) 1207–1214.

[3] T. P. Fries, A corrected XFEM approximation without problems in blending elements, International Journal for Numerical Methods in Engineering 75 (2007) 503–532.

[4] I. Babuška, U. Banerjee, Stable Generalized Finite Element Method (SGFEM), Computer Methods in Applied Mechanics and Engineering 201 (2012) 91–111. arXiv:1104.0960.

[5] V. Gupta, C. A. Duarte, I. Babuška, U. Banerjee, A stable and optimally convergent generalized FEM (SGFEM) for linear elastic fracture mechanics, Computer Methods in Applied Mechanics and Engineering 266 (2013) 23–39.

[6] W. Bangerth, R. Hartmann, G. Kanschat, deal.II – a general purpose object oriented finite element library, ACM Trans. Math. Softw. 33 (4) (2007) 24/1–24/27.